Viscosity measurements of bridgmanite by *in situ* stress and strain observations

The Earth's mantle, which is a layer of silicate rock between the crust and the metallic core, is convective, which causes the volcanic and seismic activities and thermal evolution of the Earth through plate subduction and hot plumes. Our knowledge of the rheological properties of mantle constituent minerals, including viscosity, is fundamental to comprehending the dynamics of the Earth's mantle. The Earth's mantle consists of the upper mantle (depth: >410 km), transition zone (depth: 410–660 km) and lower mantle (depth: 660–2900 km), which were distinguished by seismological and mineralogical studies. The lower mantle occupies ~65 vol% of the Earth's mantle. The viscosity-depth models of the Earth's mantle proposed on the basis of many geophysical observations [e.g., 1,2] indicate that the lower mantle has the highest viscosity, which is assumed to be 10^{19}–10^{21} Pa·s, among all the mantle layers. In addition, the viscosity difference between the transition zone and the top of the lower mantle has been assessed to be 1–2 orders of magnitude. Therefore, it is important to know the viscosity of the Earth's lower mantle to understand the Earth's mantle dynamics.

In the pyloritic mantle model, the lower mantle constituent minerals are bridgmanite (77 vol%), which is (Mg,Fe)SiO_3 perovskite with the space group *Pbnm*, ferropericlase (16 vol%) and $CaSiO_3$ perovskite (7%). The contribution of $CaSiO_3$ perovskite to viscosity is negligible because of the low abundance in the lower mantle. The viscosity of ferropericlase is considered to be much lower than that of bridgmanite. If an interconnected weak layer of ferropericlase was formed by a large shear strain such as a shear in a localized area, ferropericlase could be the dominant contributor to the lower mantle viscosity. In other cases, bridgmanite would govern the lower mantle viscosity because it is the most abundant mineral in the lower mantle.

In the Earth's mantle, the dominant deformation mechanisms are generally considered to be diffusion creep and/or dislocation creep. The total strain (ε_{total}) during deformation is the sum of the strains of diffusion creep (ε_{dif}) and dislocation creep (ε_{dis}), and viscosity (η) is defined as $\eta = \sigma/\dot{\varepsilon}_{total}$, where σ and $\dot{\varepsilon}_{total}$ are the stress and total strain rate, respectively. The diffusion creep of bridgmanite has been studied mainly by diffusion experiments under deep mantle conditions, whereas the dislocation creep of bridgmanite is still unclear. Therefore, it is essential to quantitatively investigate the flow laws of mantle minerals in the dislocation creep regime through direct measurements. To determine the viscosity of bridgmanite in the dislocation creep region, the *in situ* stress and strain measurements of $MgSiO_3$ bridgmanite during uniaxial deformation at temperatures of 1473–1673 K and pressures of 23–27 GPa were conducted using the Kawai-type cell assembly with both the deformation-DIA-type apparatus (D-DIA), which was called "KATD," at SPring-8 **BL04B1** and the deformation-111 (D111)-type apparatus at KEK, PF-AR, NE7A [3]. Stress and strain rate in the deformation experiments are under conditions of 0.25 to 4.5 GPa and 1.6×10^{-6} to 1.5×10^{-4} s^{-1}, respectively. The maximum strain of bridgmanite using KATD was 6.8% (Fig. 1), whereas it reached 30.1% using the D111-type apparatus.

Figure 2 shows the creep strengths in the dislocation creep of bridgmanite and other mantle minerals obtained in the uniaxial deformation geometry in the D-DIA apparatus. These creep strength data were obtained under nominally dry conditions, although ringwoodite and wadsleyite, which are olivine polymorphs at the mantle transition zone, contained small amounts of water (0.029–0.1 wt%). The creep strength of bridgmanite is the highest among those of olivine, its high-pressure polymorphs, and periclase. This result is also supported by the additional experiment on deformation in a serial arrangement of bridgmanite and ringwoodite along the deformation axis using KATD to observe the direct viscosity contrast between them under nominally dry conditions [3]. Quantitatively, Fig. 2 shows that the creep strength of bridgmanite is approximately one order of magnitude larger than that of ringwoodite. Therefore, the observed viscosity variation between the mantle transition zone and the top of the lower mantle would be explained by the creep strength

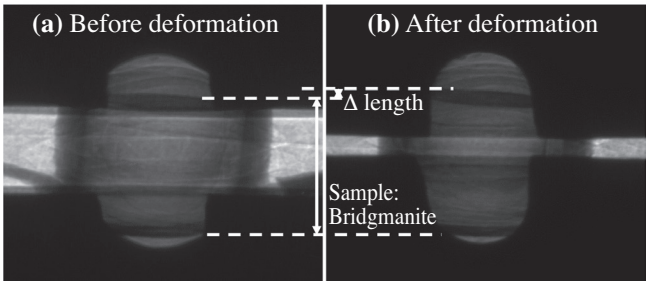

Fig. 1. X-ray radiographs before deformation **(a)** and after deformation **(b)** in M2344 using KATD. Total strain was 6.8%. Δ length is the difference between the sample lengths obtained before and during deformation.

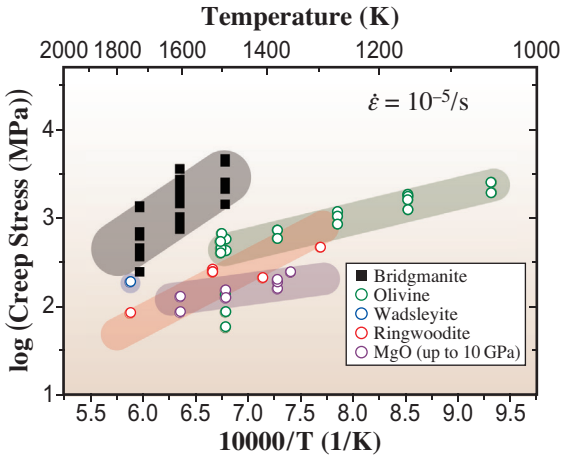

Fig. 2. Creep strength of bridgmanite at strain rate of 10^5/s in dislocation creep and those of other mantle minerals determined using the D-DIA-type apparatus. Solid black squares represent the strength of bridgmanite. Open green, blue, red and purple circles show the strengths of olivine, wadsleyite, ringwoodite and MgO, respectively.

contrast between bridgmanite and ringwoodite in the dislocation creep region even under nominally dry conditions.

The deformation mechanism map of bridgmanite at 1900 K and 25 GPa shown in Fig. 3 was also constructed using the flow law of the dislocation creep of bridgmanite [3] and the diffusion coefficients reported by annealing experiments [4] for diffusion creep. The temperature dependence of the strain rate is mainly derived from those of lattice and grain-boundary diffusion coefficients, which are the most important parameters in the diffusion creep regime. To realize a viscosity of 10^{21}–10^{22} Pa·s for the top of the lower mantle, the stress magnitude and strain rate are required to be 2×10^4 to 3×10^5 Pa and 2×10^{-18} to 3×10^{-16} s^{-1} in the grain-size-insensitive dislocation creep regime, respectively, whereas a grain size of 3–8 mm is necessary in the stress-independent diffusion creep regime shown as the yellow region in Fig. 3. These stress magnitudes of bridgmanite are consistent with those in the upper mantle estimated from the flow laws of olivine. Therefore, it is concluded that the rheology of the lower mantle is dominated by bridgmanite, which means that bridgmanite forms the load-bearing framework in the lower mantle rocks to control the lower mantle viscosity.

It is considered that the depth dependence of the diffusion coefficient for bridgmanite calculated by homologous temperature scaling with the adiabatic temperature gradient is consistent with the depth profiles of the observed lower mantle viscosity. Therefore, the observed viscosity profiles of the whole lower mantle can be explained by that of bridgmanite with constant stress and grain size conditions that correspond to the yellow region in Fig. 3. The required grain size of bridgmanite in the whole lower mantle is found to be several millimeters from the deformation mechanism map of bridgmanite. On the other hand, the grain size of bridgmanite after phase transition from the transition zone with a normal geotherm is estimated to be less than several hundred micrometers even over one billion years [5], because the grain growth rate of bridgmanite in a multiphase system is characteristically reduced. This indicates that the lower mantle materials, which have viscosities comparable to that of the lower mantle, would not have experienced the phase transition during mantle convection. Therefore, the main portion of the lower mantle would have been isolated from mixing by mantle stirring after crystallization from the magma ocean and remained as an ancient mantle.

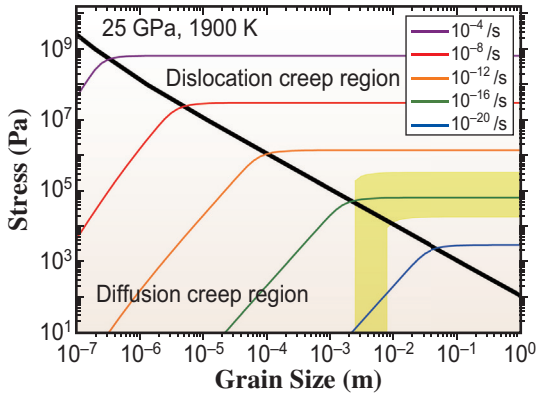

Fig. 3. Deformation mechanism maps for bridgmanite at 25 GPa and 1900 K with stress exponent n of 3 constructed using the parameters for dislocation creep [3] and diffusion creep [4]. The yellow area denotes the region dominated by diffusion creep and dislocation creep with an observed viscosity range of 10^{21}–10^{22} Pa·s.

Noriyoshi Tsujino

Japan Synchrotron Radiation Research Institute (JASRI)

Email: noriyoshi.tsujino@spring8.or.jp

References

[1] Y. Ricard, B. Wuming: Geophys. J. Int. **105** (1991) 561.
[2] J. X. Mitrovica, A. M. Forte: Earth Planet. Sci. Lett. **225** (2004) 177.
[3] *N. Tsujino, D. Yamazaki, Y. Nishihara, T. Yoshino, Y. Higo, Y. Tange: Sci. Adv. **8** (2022) eabm1821.*
[4] D. Yamazaki *et al.*: Phys. Earth Planet. Int. **119** (2000) 299.
[5] D. Yamazaki *et al.*: Science **274** (1996)2052.